Title: Assessing the Environmental Performance of NADH Regeneration Methods: A Cleaner Process using Recyclable Pt/Fe_3O_4 and Hydrogen

Authors: Tony Saba, Joseph W.H. Burnett, Jianwei Li, Xiaonan Wang, James A. Anderson, Panagiotis N. Kechagiopoulos, Xiaodong Wang

PII: S0920-5861(18)30951-9
DOI: https://doi.org/10.1016/j.cattod.2019.01.049
Reference: CATTOD 11920

To appear in: *Catalysis Today*

Received date: 19 October 2018
Revised date: 30 December 2018
Accepted date: 20 January 2019

Please cite this article as: Saba T, Burnett JWH, Li J, Wang X, Anderson JA, Kechagiopoulos PN, Wang X, Assessing the Environmental Performance of NADH Regeneration Methods: A Cleaner Process using Recyclable Pt/Fe_3O_4 and Hydrogen, *Catalysis Today* (2019), https://doi.org/10.1016/j.cattod.2019.01.049

Assessing the Environmental Performance of NADH Regeneration Methods: A Cleaner Process using Recyclable Pt/Fe_3O_4 and Hydrogen

Tony Saba,[a] Joseph W.H. Burnett,[a] Jianwei Li,[a] Xiaonan Wang,[b] James A. Anderson,[a] Panagiotis N. Kechagiopoulos,[a] and Xiaodong Wang[a,*]

[a]Chemical and Materials Engineering, School of Engineering, University of Aberdeen, Aberdeen AB24 3UE, Scotland, United Kingdom
[b]Department of Chemical and Biomolecular Engineering, National University of Singapore, Singapore 117585, Singapore

*corresponding author

Tel: +44(0)1224 273 956, e-mail: x.wang@abdn.ac.uk

Graphical abstract

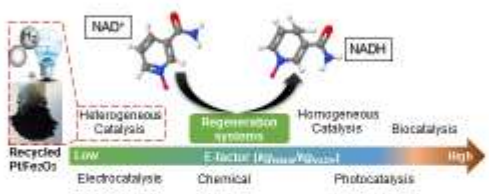

Highlights

- NAD(P)H regeneration cleanliness is crucial for sustainable biotransformations
- First assessment of environmental impact of NAD(P)H regeneration methods
- Heterogeneous catalysis and electrocatalysis produce the lowest amount of waste
- Recyclable heterogeneous Pt/Fe_3O_4 catalyst exhibits an E-factor of ~1 using H_2

Abstract

Cofactor (reduced) Nicotinamide Adenine Dinucleotide (NAD(P)H) is an energy carrier in enzymatic redox reactions that are employed for the synthesis of valuable chemicals and pharmaceuticals. The high cost of NAD(P)H makes it impractical to use in stoichiometric amounts in industrial processes. This has led to the development of a

variety of methods for NAD(P)H regeneration. In this work, process cleanliness of the current NADH recycling systems was evaluated using E-factor (kg_{waste}/kg_{NADH}) as a green chemistry metric. The E-factor obtained, depending on the process method, reaches values higher than 20000, where non-recyclable agents, including sacrificial hydride/electron donors, catalysts and electron mediators, alongside by-products (from cosubstrates), account for the overall waste. A promising alternative methodology for NADH regeneration using H_2 and recyclable Pt/Fe_3O_4 is presented and characterisation performed by temperature-programmed reduction (TPR), nitrogen adsorption (surface area/porosity), powder X-ray diffraction (XRD) and transmission electron microscopy (TEM) is used to elucidate observed performance. The Pt/Fe_3O_4 system at room temperature delivers a turnover frequency of 20 h^{-1} and the catalyst can be recycled for reuse, producing a significantly low level of waste (E-factor = ~1).

1. Introduction

Biocatalysis has been extensively used in the pharmaceutical industry for the production of chiral intermediates in the manufacture of drugs [1]. At the beginning of the 3rd millennium, biocatalysis contributed $100 billion in revenue to the chiral drug market [2]. For instance, Pfizer generated global sales of $11.9 [1] and $3.06 billion [3] after the release of its two major drugs, Lipitor (atorvastatin) and Lyrica (pregabalin), respectively, in 2010. Reduction of hydroxyketone to *cis*-diol intermediate is the key step in the synthesis of atorvastatin and it is promoted by alcohol dehydrogenase (ADH) [3]. ADH, like most of the oxidoreductase enzymes, depends on an expensive cofactor (reduced) Nicotinamide Adenine Dinucleotide NAD(P)H, to donate hydride to the substrate. Due to the major cost of NAD(P)H (NADH: $2600/mol and NADPH: $70,000/mol) [4], its stoichiometric supply in bioreductive transformations is deemed impractical.

The development of efficient and economical methods for NAD(P)H regeneration with non-expensive reducing equivalents has been an area of extensive research over the past ~40 years. Methods exploited include biocatalytic (using enzymes [5, 6] and whole cells [7, 8]), chemical (using dihydroprydine salts [9]), electrochemical (using Ti, Ni, Co, and Cd bare electrodes [10], modified gold amalgam electrode [11], and glassy carbon supported Pt and Ni electrodes [12]), photocatalytic (using carbon nitride C_3N_4 [13, 14] and doped TiO_2 catalysts [15, 16]), homogeneous catalytic (using Rh, Ir and Ru organometallic catalysts [17-19]) and heterogeneous catalytic (using supported metal catalysts [20, 21]) approaches. The success of a regenerative system was defined by Weckbecker et al. [22] by the high selectivity, stability, ease of separation, avoidance of side reactions and minimisation of byproduct(s) formation. While the performance of activity (or yield) and selectivity has been well documented and the

subject of regular reviews [21-26], there is a lack of assessment of the environmental impact (i.e., byproduct(s)/waste(s) formation with potential separation and cost issues) associated with the application of these six regeneration methods. Hollman et al, have indicated that in biocatalytic NAD(P)H regeneration systems the use of excessive amounts of substrates accumulate in the reaction medium as waste and that the hydrogenase-promoted reactions are environmentally friendly [27, 28]. Sustainability is of particular importance to the pharmaceutical sector where the negative environmental impact has already been highlighted since the 1990s: the process efficiency is very low and waste to product ratio is extremely high [29]. With ever raising awareness of “Responsible Consumption and Production” as published in the “17 Sustainable Development Goals” by the United Nations, it is imperative to understand how sustainable the production pattern is in the methods of NAD(P)H regeneration (and further the biosynthesis of chemicals/pharmaceuticals).

In this work, the environmental performance of the existing approaches of NADH regeneration is systematically examined by employing Environmental Factor (E-factor, kg of waste per kg of desired product) as a widely used green chemistry metric [30, 31]. It is demonstrated that the utilisation of a recyclable heterogeneous catalyst based on magnetite (Fe_3O_4) supported Pt and molecular hydrogen as a reducing agent is a cleaner alternative for NADH regeneration by minimising the waste resulted from sacrificial hydride/electron donors and catalysts used.

2. Method and Experimental

2.1 E-factor Calculation

The boundary of E-factor calculations was defined as the system of NADH regeneration only, i.e., excluding the ultimate *in situ* coupling with enzymatic reductions. Typically, considerations started from the NAD^+ feed, covering all the

materials/reagents (e.g., donors, mediators, etc.) used in the regeneration reaction, and ended with NADH product stream. When multiple catalytic results are presented in the same reference, E-factor was calculated based on the highest yield achieved. In calculations and for a better comparison between various processes, mass concentration (mg mL^{-1}, based on the liquid/solvent volume) was used instead of mass according to Equation 1, where the total waste (W_{Total}, mg mL^{-1}) can be expressed by Equation 2. Solvents (i.e., pH buffers) were not considered as a waste in the comparison since these are commonly used in all regeneration systems and can largely (> 90%) be recycled [32, 33]. Hydrogen has been treated as a recyclable feedstock since recycling gas from a multiphase reactive system is well established [34, 35]. A key challenge in calculating the E-factors was indeed the extraction of useful data from the literature as the volume of reactor or reaction medium is often not provided.

$$\text{E-factor} = \frac{W_{Total}\ (\text{mg mL}^{-1})}{\text{NADH Produced (mg mL}^{-1})} \quad (1)$$

$$W_{Total} = W_{Donor} + W_{Mediator} + W_{Catalyst} + W_{Cosubstrate} + W_{Unreacted\ NAD^+} \quad (2)$$

2.2 Materials

β-Nicotinamide adenine dinucleotide hydrate (NAD^+, ≥ 96.5%), β-nicotinamide adenine dinucleotide reduced disodium salt hydrate (NADH, ≥ 94%), potassium phosphate monobasic (KH_2PO_4, ≥ 99%), potassium phosphate dibasic trihydrate ($K_2HPO_4 \cdot 3H_2O$, ≥ 99%), hexachloroplatinic acid solution (H_2PtCl_6, 8% w/w in water), nickel nitrate hexahydrate ($Ni(NO_3)_2 \cdot 6H_2O$, 99.99%), iron (III) oxide (Fe_2O_3, ⩾ 97.5%), iron (II, III) oxide (Fe_3O_4, 97%) and urea (NH_2CONH_2, ≥ 99.5%) were obtained from Sigma-Aldrich. Sodium hydroxide solution (1 M) was purchased from Fischer Scientific. All the chemicals were used as received without further purification. The H_2,

N_2, and O_2 gases of ultrahigh purity (≥ 99.99%) were supplied by BOC. All materials/chemicals were used as received without further purification.

2.3 Catalyst Preparation and Characterisation

The supported Pt catalyst was prepared by deposition-precipitation method using urea as basification agent. An aqueous solution of urea (100-fold excess) and 5 mL of H_2PtCl_6 (2.08 g L^{-1}) was added to the Fe_2O_3 (10 g) with a total volume of 400 mL. The suspension was stirred at 600 rpm and heated at 2 °C min^{-1} to 80 °C where the pH progressively increased from 2.6 to 7.1 as a result of urea decomposition:

$$NH_2\text{-}CO\text{-}NH_2 + 3\ H_2O \rightarrow 2\ NH_4^+ + 2\ OH^- + CO_2 \quad (3)$$

The resulting solid was separated by vacuum filtration, washed thoroughly with distilled water to remove any residual chlorine, and then dried in a tubular furnace in a flow of N_2 (60 mL min^{-1}) at 2 °C min^{-1} to 110 °C which was maintained for 3 h. The as prepared catalyst was ground and then reduced in 5% v/v H_2/N_2 (total flow of 40 mL min^{-1}) at 200 °C (5 °C min^{-1}) for 1 h. Upon cooling down to ambient temperature, the reduced catalyst was passivated in 1% v/v O_2/He for offline characterisation and catalysis. For comparison purposes, a 10% Ni/Fe_3O_4 catalyst was prepared by wet impregnation of Fe_3O_4 support using nickel nitrate hexahydrate as precursor. The precursor (1.09 g) was dissolved in 80 mL of distilled water. The support (2 g) was added slowly to the precursor solution under moderate stirring. The pH of the solution was then adjusted to 13 using 1 M NaOH solution. The solution was left under stirring for 24 h at ambient temperature. The catalyst was recuperated by vacuum filtration and dried overnight at 110 °C, then calcined at 400 °C under static air (5 °C min^{-1}) for 4 h and reduced in 5% v/v H_2/N_2 (total flow of 40 mL min^{-1}) at 400 °C (5 °C min^{-1}) for 1 h.

Pt content was measured by inductively coupled plasma optical emission spectrometry (Vista-PRO, Varian Inc.) from the diluted extract in HF. Temperature programmed reduction (TPR) experiments were conducted in a TPDRO 1100 (CE instruments) with a TCD detector using 5% v/v H_2/N_2. Profiles were collected over a temperature range of 40-900 °C at 5 °C min^{-1} (holding for 0.5 h at final temperature). Nitrogen adsorption-desorption isotherms were obtained using commercial automated Micromeritics Gemini VII 2390p system. Specific surface area was obtained from the adsorption isotherms using the standard BET method. Pore volume and pore size were determined by BJH analysis of desorption profiles. Transmission electron microscopy (TEM) images were taken on FEI Tecnai G2 F20 equipment. Particle size distribution was determined from TEM images by counting approximately 200 particles. X-ray diffraction (XRD) experiments were performed on a Panalytical powder X-ray diffractometer. The diffraction patterns were recorded over an angular range of $10° < 2\theta < 80°$ with a step-size of 0.02°. By comparing the XRD patterns to the ICDD files, the crystalline phases were identified.

2.4 NADH Regeneration

The hydrogenation of NAD^+ for NADH regeneration was conducted in a Parr®5500 compact reactor (with a Parr®4848 reactor controller) at 25 °C, pH = 7 and H_2 pressure of 10 atm. In a typical experiment, Pt/Fe_3O_4 (100 mg) and 50 mL 0.1 M phosphate buffered solution containing NAD^+ (1.0 mM) were loaded in the reactor. The system was flushed (three times) with N_2 (3 atm) and the temperature (25 °C) allowed to stabilise. Hydrogen gas was then introduced, the system pressurised and stirring (at 900 rpm) engaged (time $t = 0$ for reaction). A non-invasive liquid sampling system via syringe/in-line filters allowed the controlled removal of aliquots from the reactor. NADH

concentration was monitored by UV-Vis spectrophotometry (Jenway 6850) at λ = 340 nm [36]. NADH yields were calculated from:

$$\text{NADH yield (\%)} = \frac{[\text{NADH}]}{[\text{NAD}^+]_0} \times 100 \quad (4)$$

Turnover frequency was calculated based on the moles of NAD^+ converted in the 15 min of the reaction and the moles of Pt active sites using Pt dispersion obtained from TEM analysis. After each reaction, the catalyst was separated from the reaction medium by a strong external magnet and washed using warm distilled water prior to the subsequent reaction with fresh NAD^+ feed under identical conditions. Repeatability of experiments is shown by error bars generated by at least duplicate reactions.

3. Results and Discussion

3.1 Environmental Assessment of NADH Regeneration using E-factor

E-factor was first introduced by Sheldon in the early 1990s as a tool to assess the environmental impact of a manufacturing process [31]. It has thereafter been widely used in the chemical and pharmaceutical industries to examine process sustainability [37, 38]. In the chemical industry, the E-factor varies from one sector to the other in the following order: Bulk chemicals (<1 to 5), Fine chemicals (5 to >50), and Pharmaceuticals (25 to >100) [31]. Large E-factors in industry are attributed mainly to conventional stoichiometric reagents/reactions than catalysis. However, the choice of the catalyst remains critical to minimise the impact of a process on the environment. Currently there is a lack of benchmark information on the E-factor of NAD(P)H regeneration systems. Results in this section are presented in decreasing order of E-factors obtained.

Enzymatic NADH regeneration has been the only method employed at industrial scale due to the high regioselectivity of the regenerating enzymes and the corresponding

high turnover numbers [4, 39]. Unfortunately, no data was available in literature to accurately calculate the level of waste produced in this method at the industrial scale. However, an overall E-factor of 17 was reported in the manufacture of the Lyrica drug through the development of a chemoenzymatic process [40]. In NADH biocatalytic regeneration, sacrificial substrates (cosubstrates) are usually used to regenerate NADH. The choice of the substrate and the prediction of side reactions are very important for the development of a green process. On the preparative scale, biocatalytic regeneration of NADH exhibits the highest E-factor (up to 23514) among all the methods assessed (Table 1). The use of glucose as cosubstrate led to the formation of large amounts of byproducts, mainly acetoin (971 mg per mg of NADH), acetic acid (3373 mg per mg NADH), and lactic acid (3169 mg per mg of NADH), which resulted in a particularly high E-factor of 23514 with the cosubstrate accounting for 87% of the total waste (see Figure 1) [7]. Hydrogen gas was used in the presence of immobilised Alcaligenes Eutrophus cells as a method of decreasing the process waste, however authors failed to demonstrate the recyclability of these cells, which translated their high concentration (100 mg mL^{-1}) into waste giving an E-factor above 1800 [8]. In contrast, the recyclability of immobilised formate dehydrogenase (FDH) enzyme supported on an alkyl modified chitosan matrix was demonstrated [5]. Nonetheless, the dependency of FDH on a fresh solution of formate in high excess with respect to NAD^+ (*ca.* 200) in every cycle means that the integrated system is not environmentally efficient with an E-factor of 88. Continuous H_2-driven biocatalytic hydrogenation of NAD^+ using coimmobilised hydrogenase and reductase on modified carbon nanotubes has been successful at the lab scale [6], but the very limited capacity of the system (24 μL min^{-1}) poses challenges for a sustainable large-scale application.

The E-factors of existing enzymatic regeneration are evidently quite high. Sustainability must be the feature of new regeneration technologies and this has driven the investigations of other developmental methods. The application of photocatalysis (Table 2) requires a complex system that includes, in general, a combination of photocatalyst, electron mediator and electron donor/hole scavenger. Mediators have been used because of their regioselective properties. It is noteworthy that without the electron mediator, only ~50% NADH yield can be achieved [41]. Typical mediators employed are cationic pentamethylcyclopentendienyl (Cp*) rhodium bipyridine complexes $[Cp^*Rh(bpy)Cl]^+$ and $[Cp^*Rh(bpy)H_2O]^+$ which are water-soluble and difficult to recycle. They, however, only contributed up to 18% to the total waste (see Figure 1). Similar to the mediators, organic electron donors (e.g., TEOA) are also water-soluble and non-recyclable but unfortunately have to be used in stoichiometric excess (TEOA/NAD^+ molar ratio between 300 and 3350 [13, 14, 36, 41-44]). They are indeed the major waste in the photocatalytic regeneration system (accounting for 96-100% of the total waste, see Figure 1). Therefore, the dependency of photocatalyst on organic electron donors imposes an environmental problem. For instance, TEOA used with a concentration between 45 and 150 mg mL^{-1} has led to high E-factors of between 80 and 2112. Titanium dioxide (TiO_2) photocatalyst has recently widespread attention in this field as it utilises water as clean source of electrons (in contrast to TEOA), diminishing the E-factor to 7.8 - 21 [15, 16]. An exception was seen elsewhere [45] where water-soluble and non-recyclable glycerol was used as the donor at a high molar ratio to NAD^+ (*ca.* 350). The poor activity of the photocatalyst accompanied with a very low NADH yield of 1.2% produced a massive E-factor of 6493. The yield of NADH indeed played a role in shifting E-factors [13, 14, 36, 41-44], but this would not be an issue in the ultimate biotransformations as NAD^+ will be continuously consumed

(i.e., no “unreacted” NAD^+ as treated in the E-factor calculations). It is worth mentioning that photocatalyst becomes the predominant waste (61-84% of total waste) when water is used as an electron donor as shown in Figure 1.

In homogenous catalysis (Table 3), the main contributor to waste is the hydride donor (usually sodium formate) that is used in high excess with respect to NAD^+ (sodium formate/NAD^+ molar ratios up to 600) [17-19, 46, 47]. In line with photocatalysis, the less the hydride donor used, the lower the E-factor obtained [17-19, 47]. Cyclometalated iridium complex was used to catalyse the reduction of NAD^+ to NADH by a different hydrogen source, ethanol. The use of the latter at a high concentration of 65 mg mL^{-1} (ethanol/NAD^+ molar ratio >12500) produced an unacceptable level of waste (E-factor of 1488) [48]. Alternatively, substituting the sodium formate and ethanol by molecular hydrogen [49] was much more effective, as it led to very low waste generation (E-factor < 1) with the water-soluble catalyst as the major waste (see Figure 1). Homogeneous catalysis may suffer from the problem of catalyst recovery, mutual deactivation with enzymes and/or possible product contamination from residues [31]. Therefore immobilised organometallic rhodium complex has been considered and applied in the regeneration of NADH with sodium formate as hydrogen source [46]. However, leaching of the active compound into the reaction medium was evident making the method impractical. Nevertheless, the process exhibits an E-factor of 61.

NADH chemical regeneration (Table 4) was achieved a long time ago via dihydroprydine compounds as direct reducing agents in excess with respect to NAD^+ (dihydropyridine/NAD^+ molar ratio between 52 and 65) [9] generating an E-factor from 15 to 19. Salts account for 100% of total waste in the chemical regeneration method

(See Figure 1) and their impossible recovery/recyclability prevents them from being a strong candidate at industrial scale [50].

Direct electrochemical regeneration of NADH (Table 5) using bare electrodes can be seen as an attractive route due to its simplicity, relative cheapness, and has been the most environmentally friendly approach (E-factor less than 1) [10-12, 51, 52]. However, historically its application to industrial level has been held back due to formation of dimers and non-enzymatically active forms of NAD(P)H [53]. The unreacted NAD^+ as a major waste (30-43%) (see Figure 1) suggests low activity of electrochemical regeneration. Mediators in indirect chemical regeneration are considered as waste (24 to 100% of total waste) because there are no reports of successful recycling [54-57]. Immobilisation of the mediator via covalent bonding at the surface of a carbon-based porous electrode has been reported [58], yet the authors only demonstrated the stability of this system over 39 h without putting its recyclability to the test. The system has a maximum yield of 43% with E-factor of 1.3.

As an alternative to the above techniques, a sixth regeneration method using heterogeneous catalysis, i.e., supported metals (Pt, Rh, Ru, Pd, Au and Ni), and hydrogen as reducing agent was recently reported by our group [20, 21]. The system can be operated in tandem with enzymatic (ADH) reduction [20] and has great potential for a cleaner and more convenient process (with straightforward downstream separation and forming H^+ as sole by-product) [59]. The E-factor obtained was 2.0 approaching that of the electrocatalytic regeneration, but the separation/recyclability was not experimentally demonstrated.

In summary, the key improvements across all methods of NADH regeneration would be to use hydrogen gas as the sole hydride donor and recyclable catalysts.

Additionally, the use of organic electron mediators and excess reagents/donors should be minimized where possible.

3.2 NADH Regeneration over Pt/Fe_3O_4 Catalyst

Magnetic catalysts have recently gained remarkable attention in heterogeneous catalysis thanks to their paramagnetic properties which make them easily recovered and hence decrease the operational costs [60-62]. Given the pertinent findings from the E-factor analysis above, the use of Pt/Fe_3O_4 as a recyclable catalyst for NADH regeneration was considered.

The TRP profiles of the γ-Fe_2O_3 support and as prepared Pt/Fe_2O_3 catalyst are presented in Figure 2. The support itself shows a broad peak between 300 and 400 °C with a hydrogen consumption of 2.01 mmol g^{-1} attributed to the reduction of Fe_2O_3 to Fe_3O_4 [63] according to the following reaction:

$$3\ Fe_2O_3 + H_2 \rightarrow 2\ Fe_3O_4 + H_2O \quad (5)$$

The as prepared catalyst shows a single positive peak at around 200 °C that is consistent with the literature where reduction peaks between 180 and 240 °C have been reported [64] for reduction of Pt species and the Fe_2O_3 support. Hydrogen consumption (2.58 mmol g^{-1}) was much greater than the amount required for stoichiometric reduction of Pt^{4+} species (0.13 mmol g^{-1}), suggesting that Fe_2O_3 was also partially reduced (*ca.* 75%) to Fe_3O_4. This reduction behaviour is in line with previous studies of Fe_2O_3 supported Pt catalysts [65, 66] and is attributed to the spillover of dissociatively adsorbed hydrogen on Pt atoms to the oxide surface. The increase in hydrogen consumption above 400 °C in the support and as prepared catalyst indicates the reduction of Fe_3O_4 to FeO and bulk phase Fe_2O_3 to Fe_xO_y and metallic Fe [65]. A reduction temperature of 200 °C was thus selected to treat the sample prior to catalysis. On the other hand, the TPR of the calcined Ni catalyst

exhibited a broad peak between 350 and 400 °C (data not shown), characteristic of the reduction of both NiO and Fe_2O_3 phases. As a result, the catalyst was reduced at 400 °C. The isothermal N_2 sorption analysis was used to determine the porous features of the Pt catalyst and the results are shown in Figure 3. The data show type IV isotherms with a loop characteristic of uniform mesoporous materials. According to the BJH pore size distribution (inset in Figure 3), the mean pore size of the Pt catalyst is 29.7 nm which agrees well with the reported literature for similar materials [67]. The specific BET surface area of the catalyst was also evaluated to be 28 m^2 g^{-1}.

The XRD patterns of Fe_2O_3 support, (as prepared) Pt/Fe_2O_3 and (reduced) Pt/Fe_3O_4 are shown in Figure 4. The diffraction peaks, at 2θ = 15°, 18.4°, 23.8°, 26.1°, 30.3°, 35.6°, 37.3°, 43.3°, 53.8°, 57.3°, 62.9°, 71.4° and 74.5° [68], are associated with the γ-Fe_2O_3 phase which is present in both the support and the as prepared catalyst. It is to take care on the fact that the crystal structure of γ-Fe_2O_3 is similar to that of Fe_3O_4 and the diffraction peaks from Fe_3O_4 nearly overlap with those from γ-Fe_2O_3 [69]. The disappearance of peaks at 23.8° and 26.1° and the increase in the intensity of the peak at 18.3°, however, prove the formation of the Fe_3O_4 phase in the reduced catalyst, in agreement with both the TPR results and the literature [68]. This reduction is also evident by the colour change of the catalyst from brownish-red to black and the very small shift in the diffraction peaks to a lower angle side [70]. The fact that no characteristic peaks for any Pt species were observed in the XRD patterns suggests that the Pt particles are very small and highly dispersed on the surface of the support. To examine this, TEM analysis was conducted. The representative TEM image of the reduced catalyst (Figure 5) shows pseudospherical Pt particles well-dispersed on the surface of the support with a narrow size distribution (< 1–3 nm) and an average

particle size of 1.5 nm. All of the critical physicochemical properties of the reduced Pt/Fe_3O_4 are summarised in Table 6.

The viability of using Pt/Fe_3O_4 and Ni/Fe_3O_4 in the regeneration of NADH was assessed by carrying out the hydrogenation of NAD^+ batch mode. The catalytic results are depicted in Figure 6. It can be seen, under the conditions of pH 7 and ambient temperature (25 °C), that the Pt/Fe_3O_4 has outerperformed Ni/Fe_3O_4 where the latter showed negligible activity. As a result, the supported Pt catalyst has been selected to be recycled. NADH production/concentration continuously increases over the course of reaction to ~50% yield before the recycle run. The Pt catalyst was able to maintain its activity throughout the recycling process with a turnover frequency of 20 h^{-1}. The successful recycling of Pt/Fe_3O_4 resulted in an attribution of zero waste related to the catalyst use. Compared to the reported Pt/Al_2O_3 (E-factor = 2.0) [20], the Pt/Fe_3O_4 system generates an E-factor of 1.1 (45% decrease) and demonstrates again that catalyst recyclability is a key factor in the development of a green and sustainable regeneration process.

4. Conclusions

A systematic assessment of the sustainability performance of cofactor NADH regeneration methods has been conducted using E-factor as a green chemistry metric and based on an extensive review of data extracted from literature. The range of E-factors obtained varies between approaches with the following general trend: electrochemical (0.02–2.7 kg/kg) ≈ heterogeneous catalytic (1.1–2.0 kg/kg) < chemical (15–19 kg/kg) < homogeneous catalytic (0.12–1488 kg/kg) < photocatalytic (7.8–2112 kg/kg) < biocatalytic (0.90–23514 kg/kg). It has been established that sacrificial hydride/electron donors, cosubstrates, catalysts and electron mediators are the major contributors to the overall waste across all the existing methods. The use of hydrogen

along with the development of a recyclable catalytic system were identified as being the key parameters in minimising the level of waste in NADH regeneration It has been demonstrated that using Pt/Fe_3O_4 is viable for NADH regeneration with H_2. A turnover frequency of 20 h^{-1} was achieved using the Pt/Fe_3O_4 system with added benefits on catalyst recyclability/stability and waste minimisation. Results here provide benchmark information on the environmental performance of NADH regeneration, presenting a promising cleaner alternative based on the use of magnetic catalytic materials and H_2 gas.

Acknowledgements

This work was supported by The Royal Society (IES\R3\170162 and RG150001) and The Binks Trust (1225).

References

[1] U.T. Bornscheuer, G.W. Huisman, R.J. Kazlauskas, S. Lutz, J.C. Moore, K. Robins, Nature 485 (2012) 185-194.

[2] R. Porter, S. Clark, Enzymes in organic synthesis, John Wiley & Sons, 2009.

[3] J. Whittall, P.W. Sutton, Practical methods for biocatalysis and biotransformations 2, John Wiley & Sons, 2012.

[4] K. Faber, Biotransformations in Organic Chemistry, 7th Edition ed., Springer, 2018.

[5] J. Roche, K. Groenen-Serrano, O. Reynes, F. Chauvet, T. Tzedakis, Chem. Eng. J. 239 (2014) 216-225.

[6] C. Zor, H.A. Reeve, J. Quinson, L.A. Thompson, T.H. Lonsdale, F. Dillon, N. Grobert, K.A. Vincent, Chem. Comm. 53 (2017) 9839-9841.

[7] Y. Wang, L. Li, C. Ma, C. Gao, F. Tao, P. Xu, Sci. Rep. 3 (2013) 2643-2648.

[8] F. Hasumi, S. Nakamura, N. Nakada, Memoirs of Numazy College of Technology 25 (1991) 63-65.

[9] K.E. Taylor, J.B. Jones, J. Am. Chem. Soc. 98 (1976) 5689-5694.

[10] I. Ali, T. Khan, S. Omanovic, J. Mol. Catal. A: Chem. 387 (2014) 86-91.

[11] S.H. Baik, C. Kang, I.C. Jeon, S.E. Yun, Biotechnol. Tech. 13 (1999) 1-5.

[12] I. Ali, A. Gill, S. Omanovic, Chem. Eng. J. 188 (2012) 173-180.

[13] D. Yang, H. Zou, Y. Wu, J. Shi, S. Zhang, X. Wang, P. Han, Z. Tong, Z. Jiang, Ind. Eng. Chem. Res. 56 (2017) 6247-6255.

[14] X. Huang, J. Liu, Q. Yang, Y. Liu, Y. Zhu, T. Li, Y.H. Tsang, X. Zhang, RSD Adv. 6 (2016) 101974-101980.

[15] Q. Shi, D. Yang, Z. Jiang, J. Li, J. Mol. Catal. B: Enzym. 43 (2006) 44-48.

[16] D. Chen, D. Yang, Q. Wang, Z. Jiang, Ind. Eng. Chem. Res. 45 (2006) 4110-4116.

[17] S. Kim, G.Y. Lee, J. Baeg, Y. Kim, S. Kim, J. Kim, J. Phys. Chem. C 118 (2014) 25844-25852.

[18] V. Ganesan, D. Sivanesan, S. Yoon, Inorg. Chem. 56 (2017) 1366-1374.

[19] Y.K. Yan, M. Melchart, A. Habtemariam, A.F. Peacock, P.J. Sadler, J. Biol. Inorg. Chem. 11 (2006) 483-488.

[20] X. Wang, H.H.P. Yiu, ACS Catal. 6 (2016) 1880-1886.

[21] X. Wang, T. Saba, H.H.P. Yiu, R.F. Howe, J.A. Anderson, J. Shi, Chem 2 (2017) 621-654.

[22] A. Weckbecker, H. Gröger, W. Hummel, Regeneration of nicotinamide coenzymes: principles and applications for the synthesis of chiral compounds, in: Biosystems Engineering I, Springer, 2010, pp. 195-242.

[23] H.K. Chenault, E.S. Simon, G.M. Whitesides, Biotechnol. Gen. Eng. Rev. 6 (1988) 221-270.

[24] R. Wichmann, D. Vasic-Racki, Cofactor regeneration at the lab scale, in: Technology transfer in biotechnology, Springer, 2005, pp. 225-260.

[25] H. Wu, C. Tian, X. Song, C. Liu, D. Yang, Z. Jiang, Green Chem. 15 (2013) 1773-1789.

[26] T. Quinto, V. Köhler, T.R. Ward, Top. Catal. 57 (2014) 321-331.

[27] F. Hollmann, I.W. Arends, D. Holtmann, Green Chem. 13 (2011) 2285-2314.

[28] Y. Ni, D. Holtmann, F. Hollmann, ChemCatChem 6 (2014) 930-943.

[29] D. Taylor, The pharmaceutical industry and the future of drug development, in: R.E. Hester, R.M. Harrison (Eds.), Pharmaceuticals in the Environment, Royal Society of Chemistry, 2016.

[30] R.A. Sheldon, ACS Sustain. Chem. Eng. 6 (2017) 32-48.

[31] R.A. Sheldon, Chem. Comm. (2008) 3352-3365.

[32] H. Huang, S. Ramaswamy, U. Tschirner, B. Ramarao, Sep. Purif. Technol. 62 (2008) 1-21.

[33] X. Wang, F. Cárdenas-Lizana, M.A. Keane, ACS Sustain. Chem. Eng. 2 (2014) 2781-2789.

[34] N. Hallale, F. Liu, Adv. Environ. Res. 6 (2001) 81-98.

[35] R. Ramachandran, R.K. Menon, Int. J. Hydrogen Energy 23 (1998) 593-598.

[36] S.S. Bhoware, K.Y. Kim, J.A. Kim, Q. Wu, J. Kim, J. Phys. Chem. C 115 (2011) 2553-2557.

[37] A.D. Curzons, D.J. Constable, D.N. Mortimer, V.L. Cunningham, Green Chem. 3 (2001) 1-6.

[38] R.A. Sheldon, Green Chem. 9 (2007) 1273-1283.

[39] E. Brenna, Synthetic Methods for Biologically Active Molecules: Exploring the Potential of Bioreductions, John Wiley & Sons, 2013.

[40] C.A. Martinez, S. Hu, Y. Dumond, J. Tao, P. Kelleher, L. Tully, Org. Process Res. Dev. 12 (2008) 392-398.

[41] J. Liu, M. Antonietti, Energy Environ. Sci. 6 (2013) 1486-1493.

[42] R.K. Yadav, J. Baeg, G.H. Oh, N. Park, K. Kong, J. Kim, D.W. Hwang, S.K. Biswas, J. Am. Chem. Soc. 134 (2012) 11455-11461.

[43] S.H. Lee, J. Ryu, D.H. Nam, C.B. Park, Chem. Comm. 47 (2011) 4643-4645.

[44] X. Ji, C. Liu, J. Wang, Z. Su, G. Ma, S. Zhang, J. Mater. Chem. A 5 (2017) 5511-5522.

[45] M. Aresta, A. Dibenedetto, T. Baran, A. Angelini, P. Labuz, W. Macyk, Beilstein J. Org. Chem. 10 (2014) 2556-2565.

[46] M. De Torres, J. Dimroth, I.W. Arends, J. Keilitz, F. Hollmann, Molecules 17 (2012) 9835-9841.

[47] J. Canivet, G. Süss-Fink, P. Štěpnička, Eur. J. Inorg. Chem. 30 (2007) 4736-4742.

[48] Y. Maenaka, T. Suenobu, S. Fukuzumi, J. Am. Chem. Soc. 134 (2012) 9417-9427.

[49] Y. Maenaka, T. Suenobu, S. Fukuzumi, J. Am. Chem. Soc. 134 (2011) 367-374.

[50] K. Goldberg, K. Schroer, S. Lütz, A. Liese, Appl. Microbiol. Biotechnol. 76 (2007) 237-248.

[51] R. Barin, S. Rashid-Nadimi, D. Biria, M.A. Asadollahi, Electrochim. Acta 247 (2017) 1095-1102.

[52] I. Ali, N. Ullah, M.A. McArthur, S. Coulombe, S. Omanovic, Can. J. Chem. Eng. 96 (2018) 68-73.

[53] C.S. Morrison, W.B. Armiger, D.R. Dodds, J.S. Dordick, M.A. Koffas, Biotechnol. Adv. 36 (2017) 120-131.

[54] S. Kim, G. Chung, S. Kim, G. Vinothkumar, S. Yoon, K. Jung, Electrochim. Acta 210 (2016) 837-845.

[55] S. Kim, M.K. Kim, S.H. Lee, S. Yoon, K. Jung, J. Mol. Catal. B: Enzym. 102 (2014) 9-15.

[56] S. Kim, G.Y. Lee, J. Lee, E. Rajkumar, J. Baeg, J. Kim, Electrochim. Acta 96 (2013) 141-146.

[57] H. Song, S.H. Lee, K. Won, J.H. Park, J.K. Kim, H. Lee, S. Moon, D.K. Kim, C.B. Park, Angew. Chem. Int. Ed. 47 (2008) 1749-1752.

[58] L. Zhang, N. Vila, G. Kohring, A. Walcarius, M. Etienne, ACS Catal. 7 (2017) 4386-4394.

[59] S. Fukuzumi, Y. Lee, W. Nam, ChemPhotoChem 2 (2018) 121-135.

[60] Y. Ma, B. Yue, L. Yu, X. Wang, Z. Hu, Y. Fan, Y. Chen, W. Lin, Y. Lu, J. Hu, J. Phys. Chem. C 112 (2008) 472-475.

[61] Y. Jang, S. Kim, S.W. Jun, B.H. Kim, S. Hwang, I.K. Song, B.M. Kim, T. Hyeon, Chem. Comm. 47 (2011) 3601-3603.

[62] X. Zhang, L. Chen, J. Yun, X. Wang, J. Kong, J. Mater. Chem. A 5 (2017) 10986-10997.

[63] I. Aragao, J. Bueno, D. Zanchet, Applied Catalysis A: General 568 (2018) 86-94.

[64] Z. He, Q. Qian, Z. Zhang, Q. Meng, H. Zhou, Z. Jiang, B. Han, Philos. Trans. A. Math. Phys. Eng. Sci. 373 (2015) 0-6.

[65] G. Fröhlich, W.M. Sachtler, J. Chem. Soc., Faraday Trans. 94 (1998) 1339-1346.

[66] N. An, Q. Yu, G. Liu, S. Li, M. Jia, W. Zhang, J. Hazard. Mater. 186 (2011) 1392-1397.

[67] Y. Liu, J. Chung, Y. Jang, S. Mao, B.M. Kim, Y. Wang, X. Guo, ACS Appl. Mater. Interfaces 6 (2014) 1887-1892.

[68] J. Azadmanjiri, G.P. Simon, K. Suzuki, C. Selomulya, J.D. Cashion, J. Mater. Chem. 22 (2012) 617-625.

[69] F. Meshkani, M. Rezaei, Int J Hydrogen Energy 39 (2014) 16318-16328.

[70] X. Wang, M. Liang, H. Liu, Y. Wang, J. Mol. Catal. A: Chem. 273 (2007) 160-168.

[71] S. Chao, M.S. Wrighton, J. Am. Chem. Soc. 109 (1987) 5886-5888.

[72] P.K. Nath, Y. Izumi, H. Yamada, Enzyme Microb. Technol. 12 (1990) 28-32.

Table 1: E-factors in Biocatalytic NADH Regeneration.

Ref.	Conditions		Results		Waste (mg mL^{-1})							E-factor
	pH	T (°C)	NADH Yield (%)	NADH formed (mg mL^{-1})	Unreacted NAD^+	Catalyst		Mediator		Cosubstrate		
[7]	7	30	41	2.0×10^{-3}	2.8×10^{-3}	Expressed GDH Escherichia coli cell	6.00	-	-	Glucose	40.00	23514
[8]	7.5	30	20.5	0.055	0.211	Immobilised Alcaligenes in polyacrylamide gel	100	-	-	H_2	0.00	1836
[5]	7	38	24	0.080	0.252	Immobilised FDH	0.00	-	-	NaCOOH	6.80	88
[71]	8	25	47	0.313	0.352	Lipoamide dehydrogenase	0.32	Pt polymer	3.20	H_2	0.00	12
[72]	9.2	30	26	8.800	24.398	Arthtobacter strain cells	14.00	-	-	NaCOOH	34.59	8.3
[6]	6	25	67	0.223	0.109	Hydrogenase/Reductase	0.09	-	-	H_2	0.00	0.90

Table 2: E-factors in Photocatalytic NADH Regeneration.

Ref.	Conditions		Results		Waste (mg mL^{-1})						E-factor
	pH	T (°C)	NADH Yield (%)	NADH formed (mg mL^{-1})	Unreacted NAD^+	Catalyst		Mediator		e^- or H^- donor		
[45]	7	25	1.25	0.007	0.524	$Ru@TiO_2$	1.00	$[Cp^*Rh(bpy)H_2O]^{2+}$	0.24	Glycerol	41	6493
[13]	9	25	36	0.048	0.085	QD@Flake g-C_3N_4	1.00	$[Cp^*Rh(bpy)H_2O]^{2+}$	0.10	TEOA	100	2112
[14]	8	25	56	0.075	0.058	g-C_3N_4	5.00	$[Cp^*Rh(bpy)H_2O]^{2+}$	0.10	TEOA	150	2082
[36]	7	25	86	0.114	0.019	Pt-NPs	0.07	-	-	TEOA	60	525
[42]	7	25	45.5	0.121	0.145	CCGCMAQSP	0.16	$[Cp^*Rh(bpy)H_2O]^{2+}$	0.08	TEOA	60	498
[43]	7.5	25	70	0.466	0.199	$QD@SiO_2$	0.00	$[Cp^*Rh(bpy)H_2O]^{2+}$	0.10	TEOA	150	322
[41]	8	25	100	0.665	0.000	DE g-C_3N_4	5.00	$[Cp^*Rh(bpy)H_2O]^{2+}$	0.10	TEOA	150	233
[44]	7	25	84	0.599	0.106	TaS_2-PEG-GR-M	0.00	$[Cp^*Rh(phen)Cl]^+$	0.00	TEOA	45	81
[15]	7	37	34.6	0.046	0.087	P-doped TiO_2	0.80	$[Cp^*Rh(bpy)H_2O]^{2+}$	0.08	H_2O	0	21
[16]	6	25	94	0.125	0.008	5%B-doped TiO_2	0.80	$[Cp^*Rh(bpy)H_2O]^{2+}$	0.17	H_2O	0	7.8

Table 3: E-factors in Homogeneous Catalytic NADH Regeneration.

Ref.	Conditions		Results		Waste (mg mL^{-1})					E-factor
	pH	T (°C)	NADH Yield (%)	NADH formed (mg mL^{-1})	Unreacted NAD^+	Catalyst		e^- or H^- donor		
[48]	10	25	86	0.044	0.007	IrIII(Cp*)(4-(1H-pyrazol-1-yl-κN^2)-benzoate-κC^3)(H_2O)	7.9×10^{-4}	Ethanol	65.55	1488
[17]	7	25	40	0.266	0.398	$[Cp^*Rh(bpy)H_2O]^{2+}$	0.05	NaCOOH	27.20	104
[46]	7	30	100	0.166	0.000	Rh(III)-TsDPEN	0.00	NaCOOH	10.20	61
[18]	7.2	60	55	1.281	1.045	$[Cp^*Rh(5,5'\text{-}CH_2OH\text{-}bpy)Cl]^+$	1.7×10^{-3}	NaCOOH	23.80	19
[47]	7	60	100	5.324	0.000	$[(\eta5\text{-}C5Me5)Rh(NN)Cl]^+$	2.34	NaCOOH	19.60	4.1
[19]	6.8	37	100	2.196	0.000	[(g6-arene)Ru(en)Cl]PF6	0.60	NaCOOH	2.92	1.6
[49]	7.6	25	97	15.492	0.478	IrIII(Cp*)(4-(1H-pyrazol-1-yl-κN^2)-benzoate-κC^3)(H_2O)	1.32	H_2	0.00	0.12

Table 4: E-factors in NADH Chemical Regeneration.

Ref.	Conditions		Results		Waste (mg mL^{-1})			E-factor
	pH	T (°C)	NADH Yield (%)	NADH formed (mg mL^{-1})	Unreacted NAD^+	e^- or H^- donor		
[9]	7	20	100[a]	0.133	0.000	3,5-dicarboethoxy-2,6-dimethyl-1,4-dihydropyridine	2.55	19
[9]	7	20	100[a]	0.133	0.000	*N*-propyl-1,4-dihydropyridinicotinamide	2.55	19
[9]	7	20	100[a]	0.133	0.000	Sodium *N*-propyl-1,4-dihydropyridine-3-carboxylate	2.55	19
[9]	7	20	100[a]	0.166	0.000	*N*-benzyl-1,4-dihydropyridinicotinamide	2.55	15
[9]	7	20	100[a]	0.166	0.000	*N*-propyl-3-(*N,N*-dimethylcarbamoyl)-1,4-dihydropyridine	2.55	15

[a]No yield was reported in [9], 100% was assumed to establish the lowest possible E-factor.

Table 5: E-factors in Electrocatalytic NADH Regeneration.

Ref.	Conditions		Results		Waste (mg mL^{-1})					E-factor
	pH	T (°C)	NADH Yield (%)	NADH formed (mg mL^{-1})	Unreacted NAD^+	Catalyst/Electrode[a]		Mediator		
[57]	7	25	45	0.299	0.365	Glassy Carbon (GC)	-	$[Cp^*Rh(bpy)Cl]^+$	0.22	2.7
[58]	6.5	25	43	0.144	0.188	CF-CNT[b]	-	$[Cp^*Rh(bpy)Cl]^+$	0.00	1.3
[54]	6	25	100	0.166	0.000	Cu-GC	-	$[Cp^*Rh(bpy)Cl]^+$	0.11	0.65
[11]	7	25	63	0.125	0.074	CMGA[c]	-	-	-	0.59
[56]	7	25	89	0.237	0.029	Pt-NPs/Amino functionalised Indium tin oxide (ITO)	3.9×10^{-6}	$[Cp^*Rh(bpy)H_2O]^{2+}$	0.04	0.31
[55]	6	25	91	0.607	0.058	Cu bare electrode	-	$[Cp^*Rh(bpy)Cl]^+$	0.11	0.27
[51]	7	25	80	0.799	0.199	Cu foam electrode	-	-	-	0.25
[10]	5.8	22	96	0.639	0.027	Ti bare electrode	-	-	-	0.04
[52]	5.8	22	98	0.652	0.013	Ni-MWCNT[d]	-	-	-	0.02
[12]	5.8	22	100	0.665	0.000	Pt-GC	-	-	-	0.00

[a]Electrode was not considered as waste.

[b]Carbon nano-tubes functionalised carbon felt.

[c]Cholesterol-modified gold amalgam.

[d]Nickel on multi-walled carbon nanotubes.

Table 6: Physicochemical characteristics of the Pt/Fe_3O_4 catalyst.

Property	
Pt loading (%)	1.2
BET surface area ($m^2\ g^{-1}$)	28
Pore volume ($cm^3\ g^{-1}$)	0.16
Pore size (nm)	29.7
Pt particle size (nm)	1.5
Dispersion[a] (%)	74

[a]Determined based on TEM Pt particle size

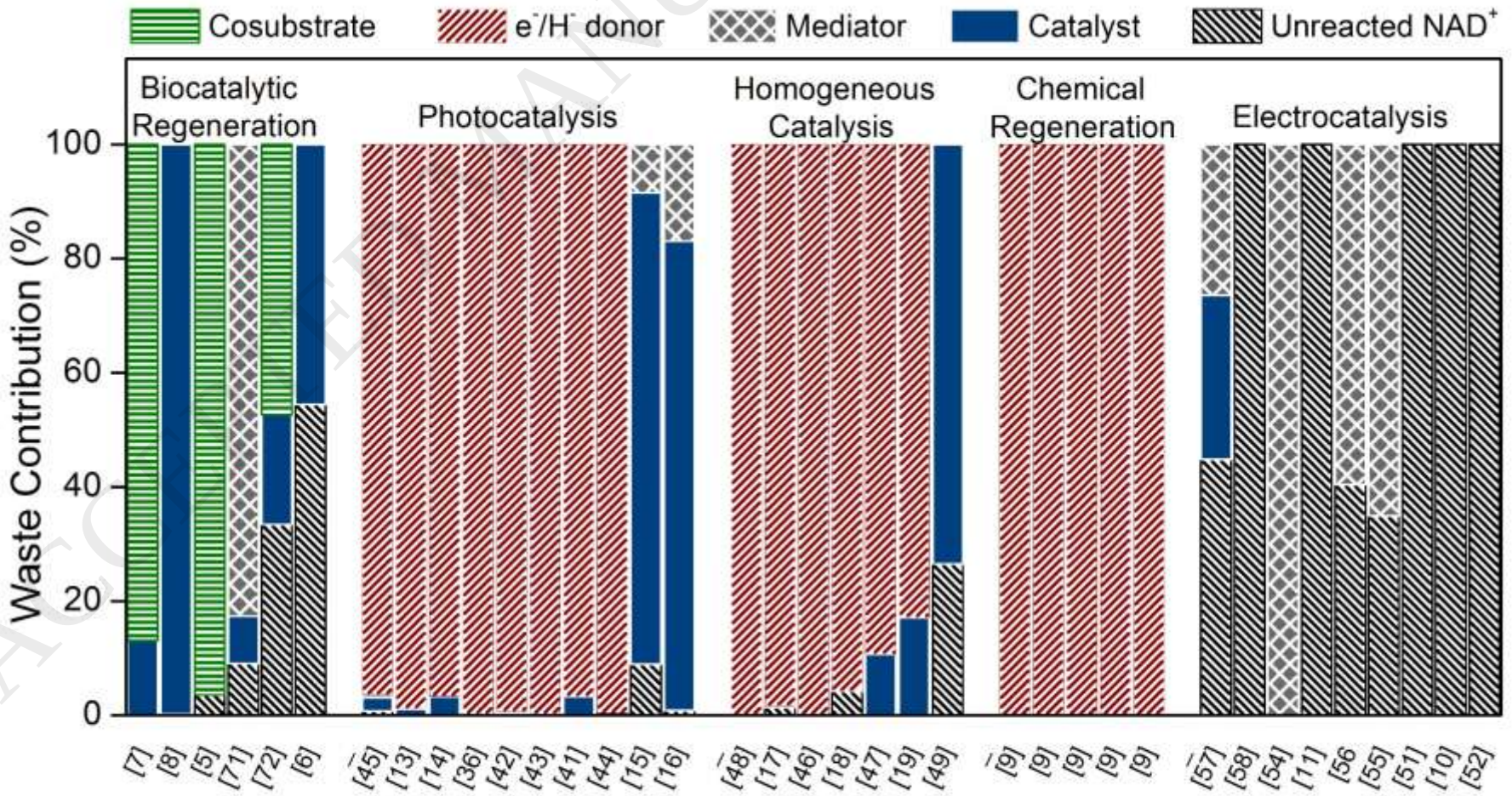

Figure 1: *Percentage of waste contribution from each component in the different NADH regeneration methods.*

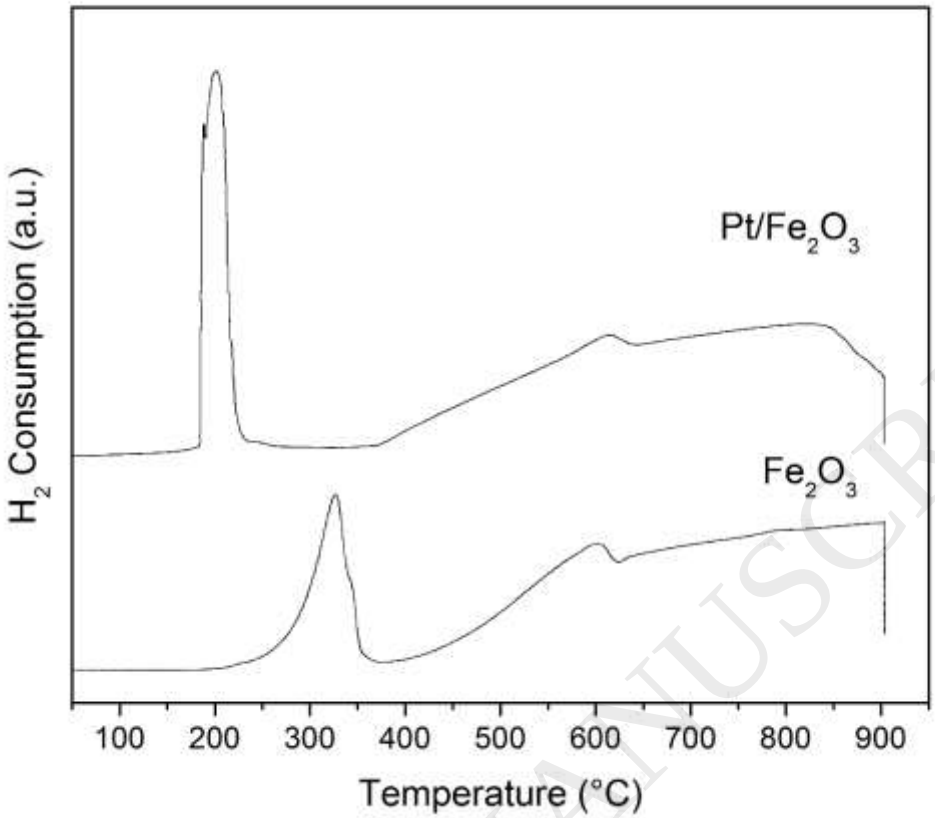

Figure 2: TPR profiles of the Fe_2O_3 support and as prepared Pt/Fe_2O_3 catalyst

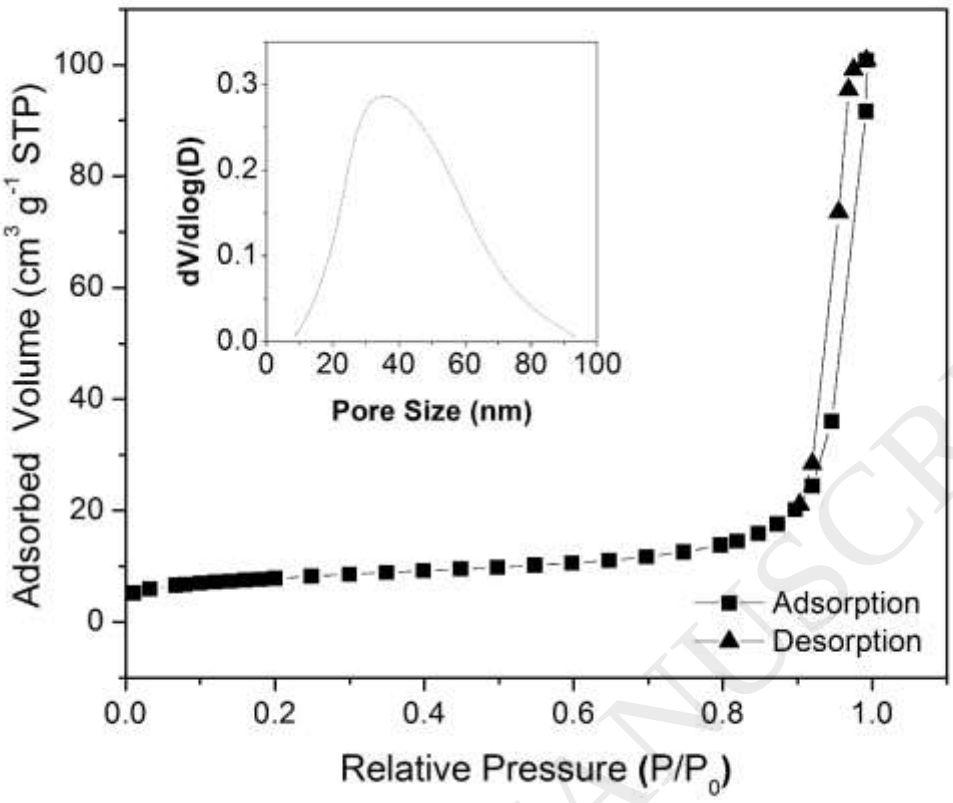

Figure 3: Isothermal N_2 adsorption-desorption curves and pore size distribution (inset) for the Pt/Fe_3O_4 catalyst.

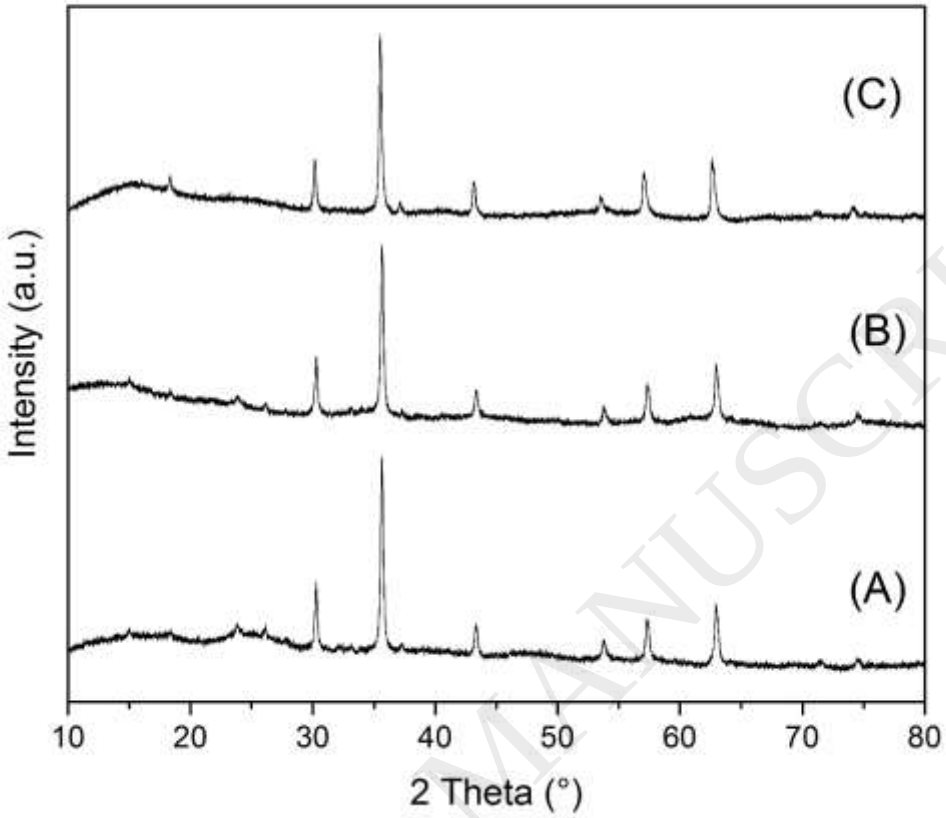

Figure 4: XRD patterns of the Fe_2O_3 support (A), as prepared Pt/Fe_2O_3 (B) and Pt/Fe_3O_4 catalyst (C).

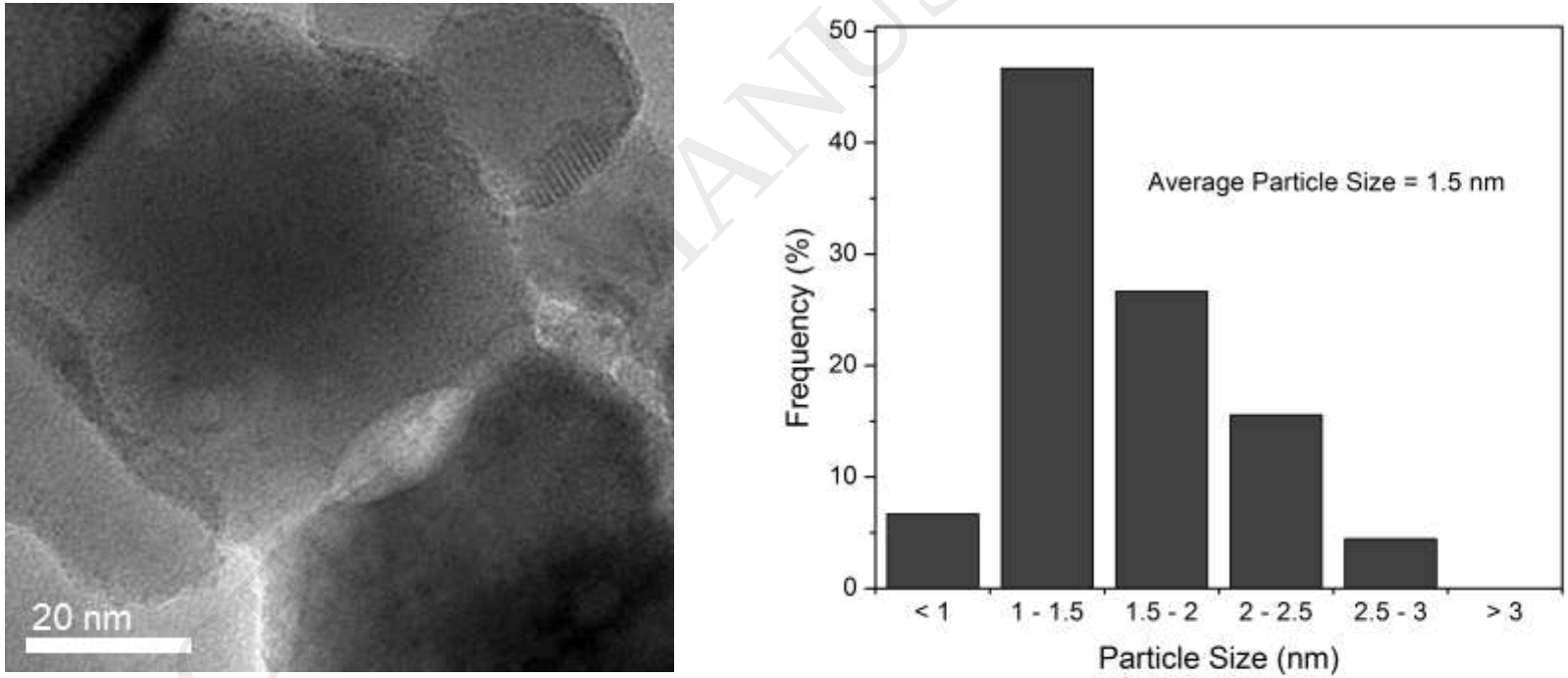

Figure 5: Representative TEM image of the Pt/Fe_3O_4 catalyst with associated particle size distribution.

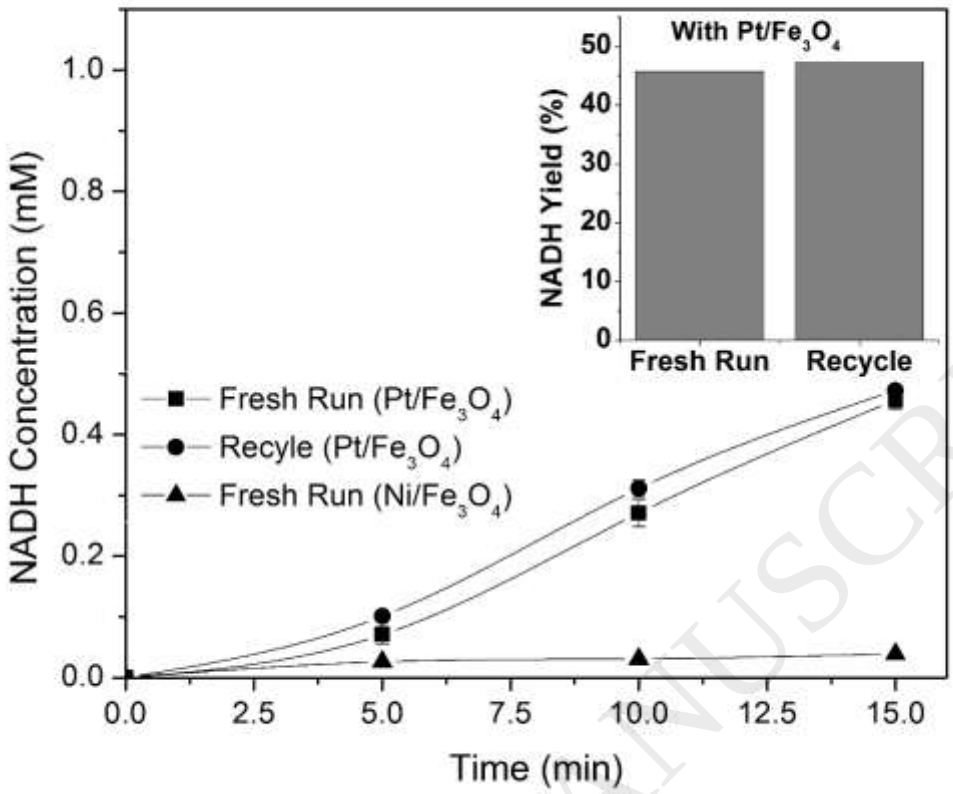

Figure 6: NADH production as a function of reaction time over the fresh/reduced Pt/Fe_3O_4 and Ni/Fe_3O_4 and recycled Pt/Fe_2O_3 catalysts (Reaction conditions: 25 °C, 10 atm, pH = 7, 900 rpm and $[NAD^+]_0$ = 1.0 mM).